Gas Processing Journal

Vol. 9, No. 2 2021, pp. 43-52
http://gpj.ui.ac.ir

Research Paper

# Energy, exergy and economic analysis of a hydrogen liquefaction process integrated with a PRICO cycle

**Arash Nourbakhsh[1], Mahdi Nami Khalilehdeh[1], Saman Faramarzi[2], Mostafa Mafi[3*]**

[1] Department of Mechanical Engineering, University of Tabriz, Tabriz
[2] Department of Mechanical Engineering, West Tehran Branch, Islamic Azad University, Tehran, Iran
[3] Department of Mechanical Engineering, Imam Khomeini International University, Qazvin, Iran

Received: 2022-02-18 Revised: 2022-04-01 Accepted: 2022-04-09

**Abstract:** Given the importance of using hydrogen fuel as one of the best sustainable energy sources, different hydrogen liquefaction technologies are developed to store and transport it over long distances. Process integration with other cycles and new high-efficiency liquefaction cycles can make hydrogen fuel more economically viable, especially for liquid hydrogen exporter countries like Iran. In this study, a hydrogen liquefaction cycle with a capacity of 1.5 tons per day is integrated with a liquefied natural gas (LNG) production process. Energy, exergy, and economic analyses are implemented to examine the proposed cycle. The novelty of this paper is based on two points: first, simultaneous production of liquefied hydrogen (LH2) and LNG in one process with an innovative configuration that leads to better performance compared to that of similar cycles, and second, simultaneous use of two-equation of states (EOS) for pure hydrogen and mixed refrigerant streams. Process integration of the LNG system with the hydrogen liquefaction unit reduces the capital expenditures (CAPEX) and operating expenses (OPEX) for both systems. Components with the greatest exergy destruction are identified. The coefficient of performance (COP) and the figure of merit (FOM) are 0.89 and 0.72, respectively. Specific energy consumption (SEC) of the proposed cycle is 5.31 kWh kg^(-1), +25 % more efficient than the similar hydrogen liquefaction cycle in the literature. The annual total cost for the proposed cycle is $35.6 million, including CAPEX, OPEX, and operation and maintenance expenditures (O&M).

**keywords:** Energy Analysis, Economic Analysis, Process integration, Efficiency, Exergy Analysis, Hydrogen.

## Highlights

- Energy, exergy, and economic analysis are performed.
- The simultaneous hydrogen and natural gas liquefaction process is proposed and developed.
- Three ortho-para hydrogen conversion reactors are located after heat exchangers.
- The specific energy consumption of the proposed cycle is 5.31 kWh $kg^{-1}$.

## 1 Introduction

Energy demand has grown significantly in recent years, and the trend is estimated to increase in the following years. Hydrogen has zero pollution in the final stage of consumption when it reacts with oxygen, and its product is water. As the most abundant component on the planet, hydrogen has always been one of the leading choices to provide clean and sustainable energy (Faramarzi et al. (2021b), (2021a); Faramarzi et al. (2021)). Hydrogen has an unavoidable role in various industries such as zero-emissions vehicles, metal coating, flat glass production, and electrical industries(Ghorbani, Ebrahimi, Rooholamini, et al. 2020; Yin and Ju 2020b). Transportation of LH2 is safer and more cost-effective than compressed-hydrogen gas; therefore, the liquefaction method is utilized to store and transport hydrogen. Although hydrogen liquefaction methods have many advantages,

* Corresponding Author.
Authors' Email Address: [1] A. Nourbakhsh (a_nourbakhsh@tabrizu.ac.ir), [2] M. Nami (mahdinami1400@ms.tabrizu.ac.ir), [3] S. Faramarzi (faramarzi.saman@wtiau.ac.ir), [4] M. Mafi (m.mafi@eng.ikiu.ac.ir)



http://10.22108/GPJ.2022.132753.1114

hydrogen liquefaction cycles consume a high rate of power, causing the price of LH2 to increase. Process integration, new design, and optimization are used to decrease the rate of energy consumption for one kilogram of LH2 (Yilmaz and Kaska 2018). Among all fuels, the highest energy value is assigned to hydrogen, approximately 140 $kJ\,kg^{-1}$ (Hosseini and Butler 2020). Power plants use natural gas to produce power, and natural gas is utilized to heat buildings, which is also utilized in *chemical* and refining *processes*. Liquefaction is an appropriate method to transport natural gas because of the low ratio of energy value to weight at ambient pressure and temperature. The most common and economical method is to reduce the natural gas temperature until it liquefies (approximately -161℃). Having liquefied, it occupies a much smaller volume (about one to six hundred) ((Zhang et al. 2020)).

Power consumption in the compression part of an LNG production cycle or a hydrogen liquefaction process has a close relationship with the price of the product, which is LNG or LH2. Consequently, it is imperative to design hydrogen and natural gas liquefaction cycles with the minimum required power. Process integration may be a solution to decrease the specific energy consumption (SEC) of natural gas and hydrogen liquefaction processes. Many countries such as Russia, Iran, Qatar, the United States, Saudi Arabia, and UAE have sizeable natural gas proven reserves and also have the potential to use hydrogen in their industries or export it; therefore, using natural gas industrial experiences in hydrogen liquefaction cycles is appropriate in an economical point of view (Sabbagh, Fanaei, and Arjomand 2020).

LNG production methods are based on three types: mixed refrigeration (MR), cascade, and expander (EXP) (Ghorbani, Zendehboudi, and Moradi 2021; Mokhatab et al. 2013). In the 1950s, Black & Veatch Company proposed the PRICO process as a simple process with low CAPEX expenditures compared to other MR LNG plants. In the PRICO process, the mixed refrigerant contains hydrocarbons and nitrogen, in turn, resulting in a better match in cold and hot composite curves in heat exchangers and also a smaller minimum temperature approach compared to pure nitrogen refrigeration cycles (Mokarizadeh Haghighi Shirazi and Mowla 2010). Linde Company proposed LIMUM1 and LIMUM3 cycles to liquefy natural gas. The LIMUM3 process includes four stages of cooling, and it is more complicated than LIMUM1. The mixed refrigerant method is used in both cycles. LIMUM1 is used in low-capacity LNG production plants, below 1600 tons per day (TPD), while LIMUM3 is appropriate for large-scale cycles (Mazyan et al. 2016). Many researchers optimized LNG production plants with mixed refrigeration systems(Faramarzi et al. 2021; Wu and Ju 2020). Morosuk et al. and Gorbani et al. (Ghorbani, Javadi, et al. 2020; Morosuk et al. 2015) investigated a PRICO process by energy, exergy, and exergoeconomic analyses. They improved the PRICO process, and they optimized the exergy-based methods. COP and energy consumptions were 0.44 and 1824 $kJ\,kg_{LNG}^{-1}$, respectively. They concluded that the design of the heat exchanger was the most effective part of LNG plants. Although the investment cost of the LNG plant increased by larger heat transfer surface in heat exchangers, minimizing exergy destruction led to a significant decrease in the total cost of the process. Aslambakhsh et al. (Aslambakhsh et al. 2018) simulated and analyzed a small-scale natural gas liquefaction unit with a capacity of 50 TPD, and they minimized the power consumption by a genetic algorithm. Lin et al. (Lin, Xiong, and Gu 2018) investigated a new high-pressure natural gas cascade cycle integrated with a new carbon dioxide cryogenic separation unit. Instead of using the conventional three-tier system, a two-cascading system was used in the new cycle. They also used three new refrigerant combinations to reduce specific energy consumption, and finally, energy analysis and thermodynamic optimization were performed on the proposed cycle. Mehrpooya *et al.* (Mehrpooya, Kalhorzadeh, and Chahartaghi 2016) developed an air separation unit and a natural gas liquid recovery cycle assisted by a nitrogen removal unit. They studied the proposed cycle by advanced exergy and exergoeconomic analyses. The irreversibility and the cost of the inefficiencies for the cycle were examined.

The first successful effort of hydrogen liquefaction was carried out by James Dewar in 1898 (Dewar 1898). Hydrogen liquefaction cycles are classified into two types, Claude and Brayton. In a Claude cycle, the expansion valve is used to reduce the temperature of hydrogen in the final stage of liquefaction, and it also adjusts the pressure of LH2, but in the reverse Brayton systems, the expansion turbine is used instead of the expansion valve. The helium Brayton cycle is suitably used to liquefy hydrogen gas in low capacity cycles below 3 TPD (Utlu and Karabuga 2021). The Claude cycle has more CAPEX and less OPEX expenditure in comparison to the Brayton cycle. Therefore, in a large capacity, the Claude method is used. Hampson–Linde, Kapitza, and mixed refrigerant cycles are used to liquefy hydrogen. Hydrogen liquefaction cycles have two main parts: pre-cooling and cooling. Mixed refrigerant or nitrogen pre-cools the hydrogen gas in the first part of the hydrogen liquefaction cycle named the pre-cooling part. In the next stage, named the cooling part, light gases like helium, hydrogen, neon, or a mixture of them are used to liquefy hydrogen (Ghorbani, Ebrahimi, Rooholamini, et al. 2020).

Growing attention to hydrogen has led many researchers to investigate various hydrogen liquefaction methods. A hydrogen liquefaction cycle was experimentally investigated by Krasae

et al. (Krasae-In et al. 2011). The pre-cooling part was performed by a mixed refrigerant consisting of several hydrocarbons, nitrogen, neon, and hydrogen, and helium gas was used as the refrigerant in the final cooling part. The components of the mixed refrigerant and the composition were guessed using temperature-pressure diagrams for different Using a mixture which was containing only hydrocarbons was also investigated. It was suggested to use nitrogen and methane in the mixed refrigerant, especially in executive projects, to increase the cooling capacity. They increased the efficiency of the cycle. Their proposed pre-cooling cycle cooled down hydrogen gas to -198 ° C. Ansarinasab et al. (Ansarinasab, Mehrpooya, and Sadeghzadeh 2019) investigated a modified hydrogen liquefaction cycle in which hydrogen gas was cooled to -195°C in the pre-cooling part. Optimization of key variables, including pressure ratio in compression unit, inlet pressure to the compressors, and minimum temperature approach in heat exchangers, was performed. Exergy, economy, and environmental analyses were utilized for the cycle. The influence of using turboexpanders and turbocompressors was studied to achieve the best performance for the proposed cycle. Wilhelmsen et al. (Berstad, Skaugen, and Wilhelmsen 2021) mathematically simulated a heat exchanger with boundary conditions that were suitable for a hydrogen liquefaction cycle. Neon gas was used to reduce the temperature difference in heat exchangers. This study indicated that the exergy destruction was caused by pressure drop, hot and cold temperature difference, and ortho-para hydrogen conversion phenomenon in hydrogen liquefaction cycles. Exergy destruction due to the pressure drop in the heat exchangers was less critical than that in other cases. At temperatures below -233℃, using a combination of neon and helium reduced the exergy destruction in heat exchangers by 43 %, but at higher temperatures, using neon or helium had little effect. Hammad and Dincer (Hammad and Dincer 2018) performed an exergy analysis for hydrogen liquefaction cycles equipped with nitrogen pre-cooling systems. The final temperature was -193℃ in the pre-cooling unit. They optimized the flow rate of the nitrogen refrigerant stream. Chang et al. (Chang, Ryu, and Baik 2018) examined low-capacity hydrogen liquefaction cycles. They used neon gas in the final cooling part of the hydrogen liquefaction cycle. Yang et al. (Yang et al. 2019) used wasted cold energy of an LNG recovery system in an LH2 production cycle. Cold energy of the LNG regasification unit was used in the pre-cooling part of a hydrogen liquefaction cycle. The capacity of the LH2 production cycle was 300 TPD. Nitrogen and mixed refrigerant gases were used in the pre-cooling and the cooling parts, respectively. The aim was to reduce the mass flow rate of the nitrogen gas stream and minimize the power consumption in the pre-cooling part. Finally, the SEC decreased from 13.58 kWh $kg^{-1}$to 11.05 kWh $kg^{-1}$. The cost of the product (LH2) was reduced from $5.13 to $2.53 per kilogram. Yin and Ju (Yin and Ju 2020a) proposed a hydrogen liquefaction cycle with a capacity of 63 kg/h. SEC, FOM, and COP were reported 7.13 kWh $kg^{-1}$, 0.17, and 0.49, respectively. The Helium refrigeration cycle was used in the cooling part of the hydrogen liquefaction cycle, while nitrogen was utilized in the pre-cooling part as the refrigerant. LH2 was liquefied at -252℃ and 300 kPa. Berstad et al. (Berstad, Stang, and Nekså 2010) performed an exergy analysis for a developed hydrogen liquefaction cycle. Claud cycle in the cooling part had 90 % of the total irreversibilities, while the mixed refrigerant pre-cooling part was responsible for 10 % of the total irreversibilities. The pre-cooling temperature was -159 ℃ and hydrogen was liquefied at -251 ℃ and 184 kPa. SEC was 6.57 kWh $kg^{-1}$. In recent years, many researchers have examined the possibility of using renewable resources in hydrogen liquefaction cycles(Rezaei et al. 2019). Aasadnia et al. (Aasadnia, Mehrpooya, and Ansarinasab 2019) investigated a cycle in which a solar energy system integrated with an absorption refrigeration cycle to pre-cool hydrogen gas. The proposed cycle with the capacity of 260 TPD had SEC and exergy efficiency values of 12.7 kWh $kg^{-1}$ and 31.6%, respectively. The highest amount of exergy destruction went to the heat exchangers located in the pre-cooling part of the hydrogen liquefaction cycle. Kaska et al. (Kaşka et al. 2018) utilized geothermal energy in an Organic Rankine power cycle to pre-cool the hydrogen gas to -30 ℃, in a Claude hydrogen liquefaction cycle. They did a thermodynamic analysis to examine the proposed cycle. Mehrpooya et al. (Mehrpooya, Sadaghiani, and Hedayat 2020) developed a hydrogen liquefaction cycle integrated with a natural gas liquefaction process. The capacity of LH2 and LNG production was 290 TPD and 296 TPD, respectively. In the proposed cycle, power consumption was 4.165 kWh $kg^{-1}$. COP and overall exergy efficiency of the proposed cycle were 24 % and 62.54%, respectively. Two ortho-para conversion reactors were implemented in the hydrogen liquefaction cycle, but temperature increase was not considered in the ortho- para conversion reactions. PR-EOS was used in their study. The temperature increases in the ortho-para conversion reactions, in turn, causing the exergy destruction to increase and the efficiency of the hydrogen liquefaction cycle decreases (Zhuzhgov et al. 2018). Consequently, the work of Mehrpooya et al. (Mehrpooya et al. 2020) mentioned above can be improved by using a more accurate equation of state in order to achieve close agreement with experimental results, especially for ortho-para conversion

reactions. Different hydrogen liquefaction cycles were investigated in the literature, but a few studies were done on low-capacity hydrogen liquefaction processes. Additionally, it has also been proven that the process of integrating can reduce the overall power consumption of the cycle, which is a point that can be further explored in the present study.

The novelty of this paper is based on the production of LNG and LH2 simultaneously, in which a new configuration for the hydrogen liquefaction cycle is proposed to achieve low operation and investment costs, resulting in low LH2 price. Three ortho-para conversion reactors are used. MBWR and PR EOSs are used to calculate thermodynamic properties. MBWR is suitable for hydrogen gas, especially in cryogenic temperatures, but the PR method is used to simulate the properties of natural gas and mixed refrigerants. Simultaneous use of two EOSs results in closer agreement with the experimental results, which is used in this study. The efficiency of the proposed cycle is compared to other research Moreover, by using economic analysis, CAPEX, OPEX, and O&M expenditures are calculated for the proposed cycle.

## 2 System description

Shown in Fig. 1 is the block flow diagram of the simultaneous LH2 and LNG production process, which is proposed in this study. Natural gas and hydrogen enter the PRICO cycle; this part not only does liquefy the natural gas but also pre-cools the hydrogen gas. LNG is the product of the PRICO cycle in which hydrogen pre-cools. LH2 is the product of the cooling part. Steam methane reforming (SMR) is used to separate hydrogen gas from natural gas. The main focus of this study is the hydrogen liquefaction cycle, and the SMR process is not within the scope of the present paper; more information about the SMR process is available in the work of Andrews (Andrews 2020).

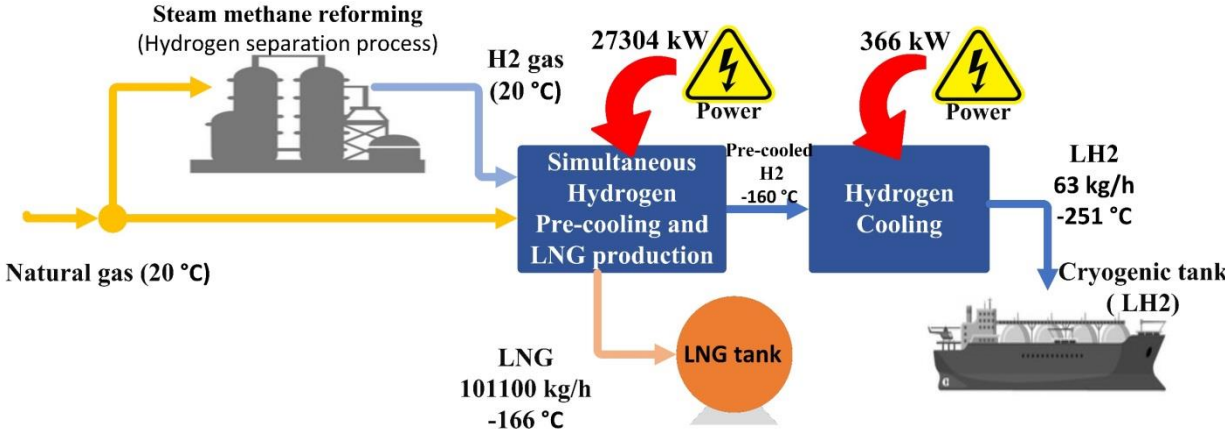


**Fig. 1. Block flow diagram of the simultaneous LH2 and LNG production cycle**

The natural gas liquefaction part named PRICO cycle is green in Fig. 2; it pre-cools hydrogen gas to -159.4 ℃. In the final part of hydrogen liquefaction named the cooling part, a combination of hydrogen, neon, and helium is used to reduce power consumption in compressors. The cooling part is shown in Fig. 2 at the top, in blue. The heat exchanger (HexM1) liquefies the incoming natural gas and pre-cools the hydrogen gas in the first stage, shown in green and orange in Fig. 2. In the cooling part, blue in Fig. 2, four heat exchangers cool down the pre-cooled hydrogen gas to -251℃. In the natural gas liquefaction section, green in Fig. 2, the cold flow stream enters the HexM1 to absorb the heat of hot streams, and it turns into gas. The pressure of this flow stream increases in the first compressor to a pressure of 1092 kPa. The increase of pressure in the compressor leads to a temperature rise. Therefore, coolers are used to cool the flow stream to 20 ℃, and it is converted into two phases liquid and gas. Passing SepM1, it separates into a liquid stream and a gas stream. A pump and a compressor increase the pressure of the separated streams to 3900 kPa. The two flow streams mix, then they cool down to 20 ° C. With M2 passing through the VM1 expansion valve, the temperature decreases to -164.3 ° C and then enters the heat exchanger (HexM1). Natural gas enters the heat exchanger (HexM1) at ambient temperature, but its pressure is 5500 kPa, and it cools down to -159 ° C. After passing the VM2 expansion valve, it reaches atmospheric pressure and then enters the separator. This process is known as the PRICO cycle (Marmolejo-Correa and Gundersen 2012). Turning to the detail of the hydrogen liquefaction process, the hydrogen gas enters the heat exchanger (HexM1) at an ambient temperature and pressure of 2400 kPa and it cools down to -159.4 ° C. Pre-cooled hydrogen gas enters the cooling part of the hydrogen liquefaction cycle in which the mixed refrigerant, including helium, neon, and hydrogen gases, is used to liquefy the hydrogen gas.

In this study, three reactors are utilized to

convert ortho-hydrogen to para-hydrogen. In the first ortho-para conversion reactor, the percentage of para-hydrogen increases from 25% to 49%. It rises in the second one, reaching 77%, and continues with a rise, peaking at 99%. Turbine expanders are used instead of expansion valves to increase the cycle efficiency. The proposed cycle is based on the modification of the model of Mehrpooya et al. (Mehrpooya et al. 2020). The pre-cooled hydrogen gas is cooled to -212 °C in the heat exchanger (HexC1.0). In HexC2.0, hydrogen is cooled to -227 °C. After passing HexC3.0 and HexC4.0, the hydrogen gas is cooled to -253 °C and then passes through the Va.LH2 expansion valve to experience a significant pressure drop, nose-diving to 300 kPa.

Liquid hydrogen is separated in Sep.LH2 and stored in cryogenic tanks. In the Brayton mixed refrigerant unit, four mixed refrigerant streams are responsible for the hydrogen liquefaction. According to Fig. 1, the MR11 stream is divided into four streams by a splitter at a pressure of 1100 kPa. After cooling the hydrogen gas, four mixed refrigerant streams enter the compression part to be compressed again. Shown in Table 1 are the properties of the stream in the proposed cycle. In this study, some assumptions are considered as follows:

- Steady-state and steady flow conditions are considered for the proposed process (Faramarz Ranjbar, Arash Nourbakhsh Saadabad, Mahdi Nami Khaliledeh, Saman Faramarzi 2022; Yin and Ju 2020a).
- The pressure drop through the coolers and heat exchangers is ignored (Saman Faramarzi, Seyed Mojtaba Mousavi Nainiyan, Mostafa Mafi 2021; Yin and Ju 2020a).
- The adiabatic efficiency of expanders and pumps are 85% and 80%, respectively (Yin and Ju 2020a).
- The adiabatic efficiency of compressors is 85 %, as recommended by Berstad et al. (Berstad et al. 2021).

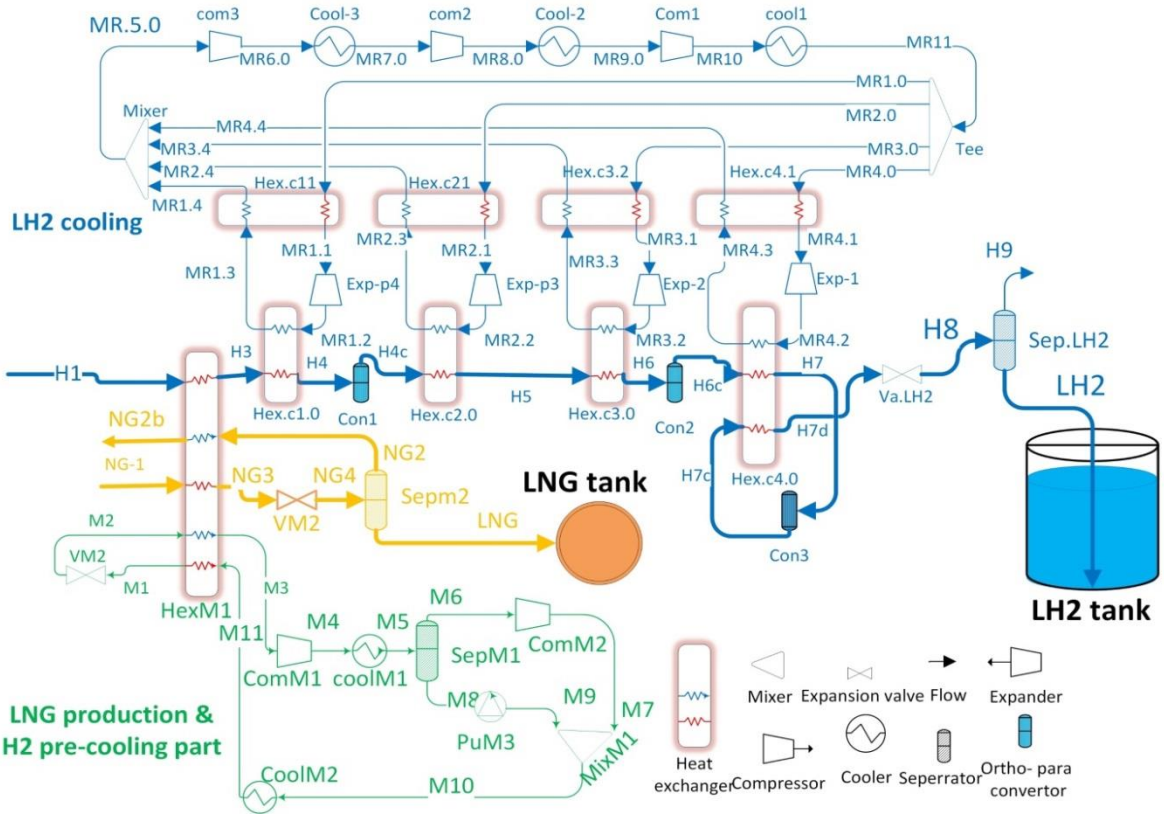


**Fig. 2. Process of the proposed cycle (deviation from reference (Faramarzi, Nainiyan, et al. 2021a)).**

**Mixed refrigerant**

The PRICO cycle is one of the simplest types of mixed refrigerant processes (Marmolejo-Correa and Gundersen 2012). Nitrogen and low boiling point hydrocarbons are used in the mixed refrigerant composition. The high rate of heat transfer coefficient for the mixed refrigerant reduces the refrigerant mass flow rate and power consumption compared to the nitrogen refrigeration cycle. On the other hand, the mixed refrigerant method increases the complexity of the process and equipment(Zhao et al. 2020); Therefore, it is necessary to choose the optimum configuration and the mixed refrigerant composition. Table 1 shows the information of main streams and the percentage of their components.

**Table 1. Stream Information of the proposed process.**

| | GH2 Feed | LH2 | LNG | NG1 | M3 | MR5.0 |
|---|---|---|---|---|---|---|
| Vapor fraction | 1 | 0 | 0 | 1 | 1 | 1 |
| Temperature/℃ | 20 | -251 | -165.7 | 20 | 10.79 | 23.44 |
| Pressure/kPa | 2400 | 300 | 101 | 5500 | 330 | 120 |
| Mass flow/ kg $h^{-1}$ | 63 | 63 | 101100 | 110000 | 450000 | 1085 |
| Percentage of the component mole fraction (%) | | | | | | |
| Hydrogen | 1.0 | 1.0 | 0 | 0 | 0 | 2.5 |
| Nitrogen | 0 | 0 | 1.5 | 4 | 13.2 | 0 |
| Methane | 0 | 0 | 89.3 | 87.5 | 21.1 | 0 |
| Neon | 0 | 0 | 0 | 0 | 0 | 33.7 |
| Propane | 0 | 0 | 2.2 | 2.1 | 16.9 | 0 |
| i-Butane | 0 | 0 | 0.3 | 0.3 | 0 | 0 |
| n-Butane | 0 | 0 | 0.6 | 0.6 | 0 | 0 |
| i-Pentane | 0 | 0 | 0.1 | 0.1 | 14.3 | 0 |
| Ethylene | 0 | 0 | 5.9 | 5.4 | 34.5 | 0 |
| Helium | 0 | 0 | 0 | 0 | 0 | 63.8 |

In the pre-cooling part, the pressure ratio is 3.3 in the first compressor, and 3.5 in the second stage, while in the final cooling section, three compression stages are performed with ratios of 2.3, 2.7, and 3.1. Heat flow, minimum temperature difference, and LMTD for heat exchangers are shown in Table 2.

**Table 2. Specifications of heat exchangers.**

| Heat exchanger | LMTD (℃) | Heat flow (kW) | Minimum temperature difference (℃) |
|---|---|---|---|
| HexM1 | 17.3 | 73118 | 1 |
| HexC1.0 | 5.3 | 2651 | 2.2 |
| HexC11 | 1.4 | 21609 | 1.1 |
| HexC2.0 | 6.2 | 1393 | 3.9 |
| HexC21 | 1.3 | 19588 | 1 |
| HexC3.0 | 5.9 | 1687 | 2.4 |
| HexC31 | 1.5 | 14301 | 1.2 |
| HexC4.0 | 6.5 | 367 | 3.3 |
| HexC4.1 | 5.6 | 10157 | 3.2 |

**Ortho-para conversion reaction**

Hydrogen contains 25% para-hydrogen and 75% ortho-hydrogen at ambient temperature. As the temperature decreases, the percentage of para-hydrogen increases. 99% para-hydrogen will be present in the hydrogen composition at the liquefaction temperature, but this reaction is exothermic, and it lasts a few days; therefore, it is an obstacle in hydrogen liquefaction cycles. Various catalysts are used to increase the rate of ortho-para conversion reaction (Yin and Ju 2020a). The released heat from the ortho-para conversion reaction is 527 kJ $kg^{-1}$, while the heat of evaporation of LH2 is 446 kJ/kg. Consequently, the liquid hydrogen will start to evaporate if it is not converted to para-hydrogen in the liquefaction process (Ram B. Gupta, Basile, and Veziroglu 2013). In this research, three ortho-para conversion reactors are used. The percentage of para-hydrogen reaches 25% in the first stage, 77% in the second stage, and 99% in the final stage. The conversion reaction rate ($r_{H2}$) is related to the catalyst reaction rate (K) and concentration of the feed hydrogen gas ($C_{H2}$), the equation is given as follows(Ghorbani et al. 2021):

$$r_{H2} = k \times C_{H2} \quad (1)$$

Where the unit of $r_{H2}$ is kmol. $(1.s^{-1})$, and the unit of $k$ and $C_{H2}$ are $s^{-1}$ and kmol, respectively. Based on the work of (Yin and Ju 2020a), $k$ is considered 1.2 $s^{-1}$and the selected catalyst is $Fe(OH)_3$.

**3 Modeling and simulation**

In this study, a commercial software named ASPEN HYSYS 11 is used to simulate the cycle. The proper EOS should be chosen by considering the temperature and pressure ranges of gases. Using suitable EOS is crucial to achieving close agreement with experimental results. Stream properties are given in Table 3. In this work, Modified Benedict-Webb-Rubin (MBWR) method, as recommended by (Valenti, MacChi, and Brioschi 2012) is used for pure hydrogen streams because this method has a better agreement with the experimental results of the work of (Jacob W. Leachman et al. 2017), especially in cryogenic temperatures. Added to this, The PR method is utilized to simulate other streams including mixed refrigerant and natural gas streams. The PR equation is derived from the Van Der Waals

relation and is a quasi-experimental state equation. The following equation shows the Peng-Robinson equation(Valenti et al. 2012):

$$P = \frac{RT}{v-b} - \frac{a\theta}{v(v+b)+b(v-b)} \quad (2)$$

$$\theta = [1 + m(1 - \sqrt{T_r}]^2$$

$$m = 0.3796 + 1.5422\omega - 0.2699\omega^2$$

More detailed information about "a" and" b" and the method of calculation of properties for gas mixtures are given in references (Ahmed 2016; M. Mafi 2015).

**Table 3. Stream properties of the proposed cycle.**

| Stream | $T$(℃) | $P$ /kPa | Mass flow/ / kg $h^{-1}$ | Mass enthalpy / kJ $kg^{-1}$ | Mass entropy/ kJ $kg^{-1}$ ℃$^{-1}$ | Stream | $T$(℃) | $P$ /kPa | Mass flow/ kg $h^{-1}$ | Mass enthalpy/ kJ $kg^{-1}$ | Mass entropy/ kJ $kg^{-1}$ ℃$^{-1}$ |
|---|---|---|---|---|---|---|---|---|---|---|---|
| H3 | -159.40 | 2400 | 63 | 1699 | 45 | MR10 | 144.36 | 1100 | 1085 | 480 | 15 |
| H4 | -212.04 | 2400 | 63 | 1061 | 37 | MR11 | 25.00 | 1100 | 1085 | 0 | 14 |
| H5 | -227.28 | 2400 | 63 | 664 | 32 | H8 | -250.98 | 300 | 63 | -225 | 9 |
| H6 | -245.01 | 2400 | 63 | 203 | 20 | LH2 | -250.98 | 300 | 63 | -225 | 9 |
| H7 | -248.00 | 2400 | 63 | -23 | 15 | H4a | -198.59 | 2400 | 63 | 1061 | 39 |
| MR1.0 | 25.00 | 1100 | 175 | 0 | 14 | H4c | -198.59 | 2400 | 63 | 1061 | 39 |
| MR1.1 | -158.00 | 1100 | 175 | -737 | 10 | H6a | -236.29 | 2400 | 63 | 203 | 22 |
| MR1.2 | -218.17 | 120 | 175 | -976 | 10 | H6c | -236.29 | 2400 | 63 | 203 | 22 |
| MR1.3 | -161.00 | 120 | 175 | -747 | 13 | H7a | -238.62 | 2400 | 63 | -23 | 15 |
| MR1.4 | 22.46 | 120 | 175 | -10 | 17 | H7c | -238.62 | 2400 | 63 | -23 | 15 |
| MR2.0 | 25.00 | 1100 | 170 | 0 | 14 | H7d | -253.02 | 2400 | 63 | -225 | 8 |
| MR2.1 | -198.00 | 1100 | 170 | -899 | 8 | LNG | -166 | 101 | 101100 | -4629 | 4 |
| MR2.2 | -237.39 | 120 | 170 | -1054 | 9 | NG3 | -159 | 5500 | 110000 | -4469 | 4 |
| MR2.3 | -200.79 | 120 | 170 | -907 | 11 | NG4 | -166 | 101 | 110000 | -4469 | 4 |
| MR2.4 | 23.01 | 120 | 170 | -8 | 17 | NG1 | 20 | 5500 | 110000 | -3711 | 8 |
| MR3.0 | 25.00 | 1100 | 320 | 0 | 14 | NG2 | -166 | 101 | 8900 | -2654 | 7 |
| MR3.1 | -225.00 | 1100 | 320 | -1010 | 6 | M1 | -160 | 3900 | 450000 | -1776 | 1 |
| MR3.2 | -250.44 | 120 | 320 | -1107 | 7 | M2 | -164 | 330 | 450000 | -1776 | 1 |
| MR3.3 | -228.00 | 120 | 320 | -1016 | 10 | M3 | 11 | 330 | 450000 | -1111 | 5 |
| MR3.4 | 23.33 | 120 | 320 | -7 | 17 | M4 | 80 | 1092 | 450000 | -1001 | 5 |
| MR4.0 | 25.00 | 1100 | 420 | 0 | 14 | M5 | 20 | 1042 | 450000 | -1177 | 4 |
| MR4.1 | -240.60 | 1100 | 420 | -1075 | 5 | M6 | 20 | 1042 | 354819 | -856 | 5 |
| MR4.2 | -253.93 | 120 | 420 | -1143 | 5 | M7 | 111 | 3900 | 354819 | -720 | 5 |
| MR4.3 | -243.50 | 120 | 420 | -1079 | 8 | M8 | 20 | 1042 | 95181 | -2377 | 1 |
| MR4.4 | 24.11 | 120 | 420 | -4 | 17 | M9 | 22 | 3900 | 95181 | -2371 | 1 |
| MR5.0 | 23.44 | 120 | 1085 | -6 | 17 | M10 | 74 | 3900 | 450000 | -1069 | 4 |
| MR6.0 | 118.68 | 230 | 1085 | 376 | 17 | M11 | 20 | 3900 | 450000 | -1291 | 4 |
| MR7.0 | 25.00 | 230 | 1085 | 0 | 16 | H1 | 20 | 2400 | 63 | 4134 | 57 |
| MR8.0 | 142.25 | 500 | 1085 | 471 | 16 | NG2b | 17 | 101 | 8900 | -2365 | 9 |
| MR9.0 | 25.00 | 500 | 1085 | 0 | 15 | | | | | | |

A comparison between the conversion enthalpy obtained from the MBWR and experimental results (Jacob W. Leachman et al. 2017) is shown in Fig. 3. Shown in Fig. 3 is the accuracy of conversion enthalpy calculation which is at least less than 1.5 % for the MBWR method. Shown in Fig. 4 is the validation of the MBWR method for the heat capacity of hydrogen in different temperatures. Results from Fig. 3 and Fig. 4 indicate that among PR, PRSV, and MBWR EOSs, MBWR is found to be the most accurate EOS for pure hydrogen streams.

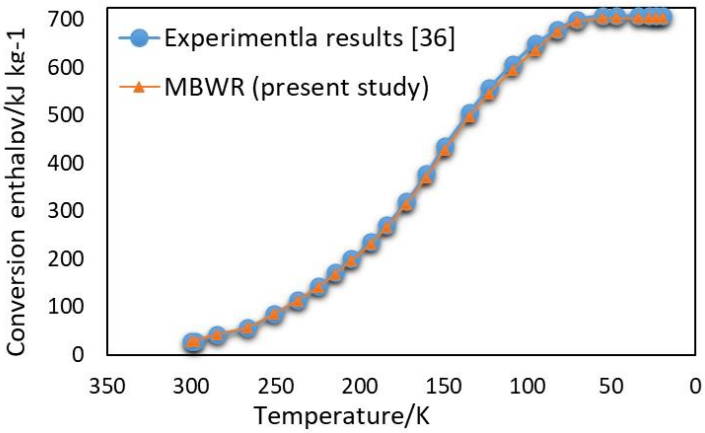


**Fig. 3. Validation of MBWR EOS for the conversion enthalpy in different temperatures.**

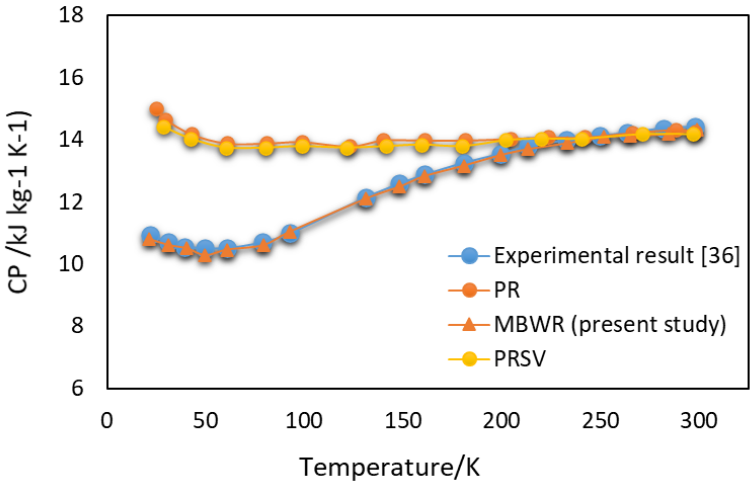


**Fig. 4. Heat capacity of hydrogen ($C_p$) calculated by different EOSs.**

able 3 shows the validation of the method used in this paper and the results of the work of (Xu et al. 2013) in which a PRICO cycle was investigated.

**Table 4. Validation of PRICO cycle with work of (Xu et al. 2013).**

| Variables | This paper | (Xu et al. 2013) |
|---|---|---|
| Minimum temperature difference (℃) | 3 | 3 |
| Specific energy consumption (SEC) | 0.280 | 0.281 |

**Thermodynamic analysis**

According to the first law of thermodynamics, considering steady-state conditions and the absence of kinetic and potential energy changes, the two equations of energy and mass balance used in this research are given as follows (Aasadnia, Mehrpooya, and Ghorbani 2021):

$$\sum \dot{m}_{in} = \sum \dot{m}_{out} \qquad (3)$$

$$\dot{Q_{cv}} + \sum \dot{m}_{in}\, h_{in} = \sum \dot{m}_{out}\, h_{out} + W_{cv}$$

Some performance parameters, such as SEC, COP, FOM, and exergy efficiency, are calculated to evaluate the system. FOM is calculated according to Equation 3 (Babu 2019). SEC evaluates the amount of electricity consumption for one kilogram of LH2 or LNG. By using Equation 4, SEC is calculated (Cardella, Decker, Sundberg, et al. 2017; M Mafi, Amidpour, and Naeynian 2009):

$$FOM = \frac{W_{rev}}{W_{ac}} = \frac{(h_l - h_0) - T_0(S_l - S_0)}{P_{net}} \qquad (4)$$

$$SEC = \frac{P_{net}}{\dot{m}_l} \qquad (5)$$

Where $W_{rev}$ is reversible work, $W_{ac}$ is real work, $h_0$ is the entropy at ambient temperature, $S_0$ is enthalpy at ambient temperature, and $S_l$ and $h_l$ are specific entropy and enthalpy of liquid gas, respectively. COP is the ratio of the heat which is taken from the cold streams in heat exchangers per the total power consumption in the cycle (Tan et al. 2018):

$$COP = \frac{Q_c}{P_{net}} \qquad (6)$$

where $Q_c$ is the heat taken from the cold streams in heat exchangers. Exergy analysis is performed for the proposed cycle, and the exergy of streams is considered as follows, excluding the changes of kinetic and potential exergy (Fratzscher 1997; M. Mafi, Naeynian, and Amidpour 2009):

$$e = e^{ph} + e^{ch} \qquad (7)$$

$$e^{ph} = h - h_0 - T(S - S_0)$$

Where $h_0$ and $S_0$ represent the enthalpy and entropy of a stream at ambient temperature and pressure, respectively.

Chemical exergy could not be neglected in the study because there is a chemical reaction in ortho-to-para reactors. Standard exergy values presented in (Kotas 1985), by using standard values for pure materials, chemical exergy of different mixtures can be calculated as follows (Kotas 1985):

$$e_m{}^{ch} = \sum_j x_j e_j{}^{ch} + \bar{R}T_0 \sum_j x_j ln x_j \qquad (8)$$

Exergy destruction is calculated using the exergy balance equation in equipment according to the following equation (Fratzscher 1997):

$$Ex_i + Ex_{Qi} = Ex_o + Ex_{Qo} + W_{sh} + I \qquad (9)$$

Irreversibility or exergy destruction is calculated by Equation 9 in which $Ex_o$ and $Ex_i$ are the exergy of the output and input streams, $Ex_{Qi}$ and $Ex_{Qo}$ are the exergy of the input and the output heat flows, $W_{sh}$ is the power consumption in the process, and $I$ is the irreversibility. The equations of exergy efficiency and exergy destruction for all equipment are given in Table 5.

**Table 5. The equations of exergy efficiency and exergy destruction for equipment.**

| Components | Exergy efficiency | Exergy destruction |
|---|---|---|
| Compressor | $\eta_{ex} = \frac{e_{in} - e_{out}}{W_{com}}$ | $I = e_i - e_o + W_{com}$ |
| Heat exchanger | $\eta_{ex} = 1 - \left\{\frac{\sum_1^n(\dot{m}\Delta e)}{\sum_1^n(\dot{m}\Delta h)}\right\}_{hot} + \left\{\frac{\sum_1^n(\dot{m}\Delta e)}{\sum_1^n(\dot{m}\Delta h)}\right\}_{cold}$ | $I = \sum(e_{in} - e_{out})$ |
| Throttle valve | $\eta_{ex} = \frac{e_{out}^{\Delta T} - e_{in}^{\Delta T}}{e_{in}^{\Delta p} - e_{out}^{\Delta p}}$ $e^{\Delta T} = (\int_T^{T_0} \frac{T - T_0}{T} dh)_p$ $= e^{\Delta T} + e^{\Delta p}$ | $I = e_{in} - e_{out}$ |
| Reactor | $\eta_{ex} = \frac{e_{out}}{e_{in}}$ | $I = e_{in} - e_{out}$ |
| Turbine expander | $\eta_{ex} = \frac{W_{tur}}{e_{in} - e_{out}}$ | $I = e_{in} - e_{out} + W_{tur}$ |
| Flash drum | $\eta_{ex} = \frac{e_0}{e_{in}}$ | $I = e_{in} - e_{out}$ |
| Reactor | $\eta_{ex} = \frac{e_{out}}{e_{in}}$ | $I = e_{in} - e_{out}$ |
| Mixer and Tee | $\eta_{ex} = \frac{e_0}{e_{in}}$ | $I = e_i - e_o$ |

The total exergy destruction and the overall exergy efficiency are calculated by Equations 14 and 15, respectively(Ghorbani, Ebrahimi, Skandarzadeh, et al. 2020; Ghorbani et al. 2021):

$$\eta_{\text{cycle}} = 1 - \frac{I_{total}}{p_{net}} \quad (14)$$

$$I_{total} = \sum_i I_i \quad (15)$$

**Economy analysis including CAPEX, OPEX, and O&M expenditures**

Devices, electricity, and feed gas expenditures are the main parts of the CAPEX and OPEX. For a better comparison, these costs are calculated annually to compare with other expenditures. Equation 16 shows CAPEX expenditure of liquefaction unit, which is based on cost factors as recommended by Couper et al. (Faramarzi, Nainiyan, et al. 2021b):

$$C_{CAPEX,t} = C_{eq}(1 + C_{ins} + C_{pip} + C_{bld} + C_{elc} + C_{stf} + C_{isu} + C_{eng} + C_{cnt} + C_{ctg} + C_{wrc}) \quad (16)$$

$$C_{eq} = (1 + c_{del})(C_{Hex} + C_{tur} + C_{com} + C_{oth}) \quad (17)$$

$c_{del}$ (cost of delivery), $C_{Hex}$ (cost of heat exchangers), $C_{com}$ (cost of compressors), $C_{tur}$ (cost of turbines), $C_{oth}$ (cost of other devices excluding heat exchangers, and compressors), $C_{ins}$ (cost of installation), $C_{pip}$ (cost of piping), $C_{bld}$ (cost of building), $C_{elc}$ (cost of control systems), $C_{stf}$ (cost of safety system), $C_{isu}$ (cost of pipelines and cold box insulation), $C_{eng}$ (cost of design and supervision), $C_{cnt}$ (cost of contracting), $C_{ctg}$( unforeseen costs), $C_{wrc}$ (cost of system testing). Cost factors are given in Table 6 , and the purchase cost of equipment is shown in Table 7.

**Table 6. Cost factors of capital expenditures (Faramarzi, Nainiyan, et al. 2021b).**

| Cost factor | Name | Value | Cost factor | Name | Value |
|---|---|---|---|---|---|
| $C_{ins}$ | Installation | 0.10 | $C_{isu}$ | Insulation | 0.10 |
| $C_{pip}$ | Piping | 0.15 | $C_{eng}$ | Engineering supervision | 0.03 |
| $C_{bld}$ | Building construction | 0.10 | $C_{cnt}$ | Contracting fee | 0.15 |
| $C_{elc}$ | Electric systems | 0.07 | $C_{ctg}$ | Unforeseen expenses | 0.10 |
| $C_{stf}$ | Safety systems | 0.03 | | | |

**Table 7. Cost of different equipment (Donaubauer et al. 2019; Faramarzi, Nainiyan, et al. 2021b; Nouri, Miansari, and Ghorbani 2020).**

| Components | Cost equation |
|---|---|
| Heat exchanger | $C_{hex} = f_{\text{p,hex}}.(8500 + 409\left(A_{Hex}\frac{UA}{f_{cry}}\right)^{0.83})$ $f_{cry}(T < 128\ K) = 0.1\ \text{kW m}^{-2}$ $f_{cry}(293\ K > T > 128\ K) = 0.2\ \text{kW m}^{-2}$ |
| Compressor | $C_{com} = 7900(\text{W}_{com})^{0.62}$ |
| turbine expander | $C_{tur} = 378(\text{W}_{tur})^{0.81}$ |
| Ortho-para conversion reactor | $C_{con} = 2860B_{con}^{0.69} + 28940V_{con}$ |
| Other components | $c_{oth} = 0.18\ (C_{hex} + C_{com} + C_{tur} + C_{con} + C_{oth})$ |

The amount of production of LNG or LH2 per year is calculated as follows (Serio et al. 2015):

$$\dot{m}_{L,\,a} = Y_a . 17280000 . \dot{m}_{LNG} \quad (18)$$

Where $\dot{m}_L$ is the mass flow of LNG or LH2 per one second. $Y_a$ is the annual rate of cycle activity, including 8322 working hours per year (Serio et al. 2015). Annual CAPEX is given as follows (Cardella, Decker, and Klein 2017; Faramarzi et al. 2021):

$$C_{CAPEX,a}=C_{CAPEX,t}.\frac{I_a.(1+I_a)^t}{(1+I_a)^t-1} \quad (19)$$

Where $t$ is the payment period in terms of the year, $I_a$ is the annual interest rate and $C_{CAPEX,t}$ represents the total initial cost. $C_{OPEX,t}$ includes the cost of electricity ($C_{el,a}$), feed gas ($C_{feed,\,a}$), and refrigerants charge ($C_{feedf,a}$) as defined below(Akrami et al. 2018; Ghorbani et al. 2019):

$$C_{OPEX,a} = C_{el,a} + C_{feed,a} + C_{feedf,a} \quad (20)$$

The cost of maintenance, compressor seals, and personnel and operation supervision are considered as $C_{O\&M,a}$ (Cardella, Decker, and Klein 2017). The cost of annual electricity is calculated as follows (Ghorbani et al. 2012):

$$C_{el} = c_{el} . \dot{m}_{L,a} . SEC \quad (21)$$

Where $c_{el}$ is the cost of electricity in kWh, and $\dot{m}_{L,a}$ is the amount of LNG or LH2 production in one year.

## 4 Results and discussion

Three cases are investigated in this study. A comparison of three cases is done in this study. Results show that Case 3 performs better than the other cases. The information, which is given in Tables 1 and Table 2, in the previous sections, is related to Case 3 (final case), because Case 3 has better performance than that the other two cases. Results show that the total power consumption for Case 3 is 27,639 kW consisting of 366 kW in cooling and 27304 kW in the pre-cooling part, and SEC for the hydrogen liquefaction cycle of Case 3 is 5.31 kWh/kg. Case 1 as the base case compares to Case 3 as the final case in Fig. 5 and Fig. 6 in terms of exergy analysis. Shown in Fig. 5 and Fig. 6 are the exergy destruction and exergy efficiency of different equipment, respectively. Results in Fig. 5 show that heat exchangers in Case 1 have a significant role in total exergy destruction. Minimum and maximum pressure in the mixed refrigerant cycle, the mass flow rate of the mixed refrigerant stream, and mixed refrigerant composition are considered key parameters to minimize the total exergy destruction, especially in heat exchangers. As shown in Fig. 5 and Fig. 6, it is crystal clear that Case 3 (final case) had a better performance than Case 1(base case).

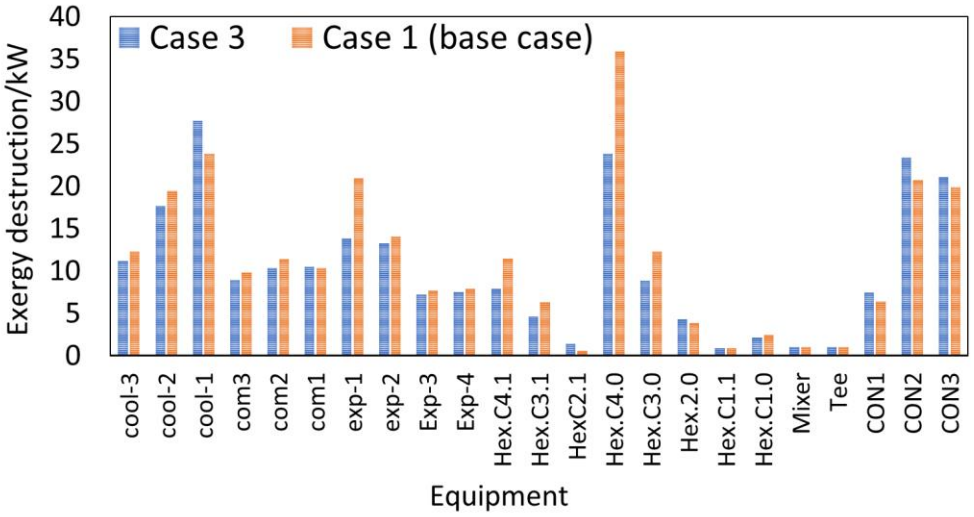


**Fig. 5.1. LH2 cooling cycle**

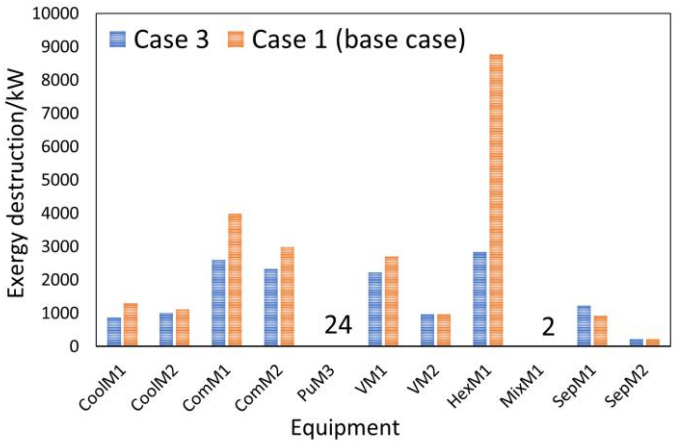


**Fig. 5.2. LNG and LH2 pre-cooling part.**

**Fig. 5. Exergy destruction in 2.1: LH2 Cooling part. 2.2: LNG or LH2 pre-cooling part.**

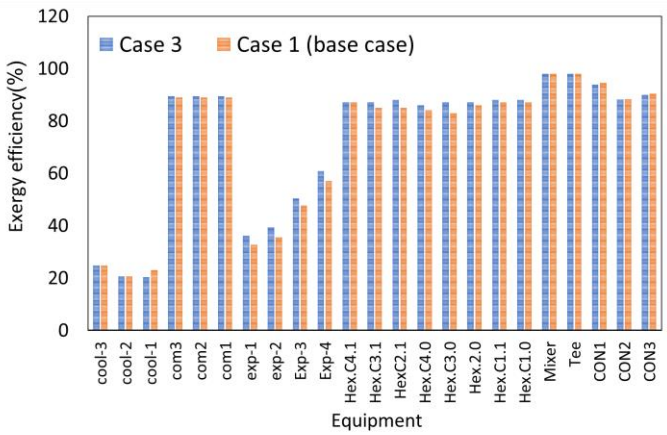


**Fig. 6.1. LH2 cooling cycle**

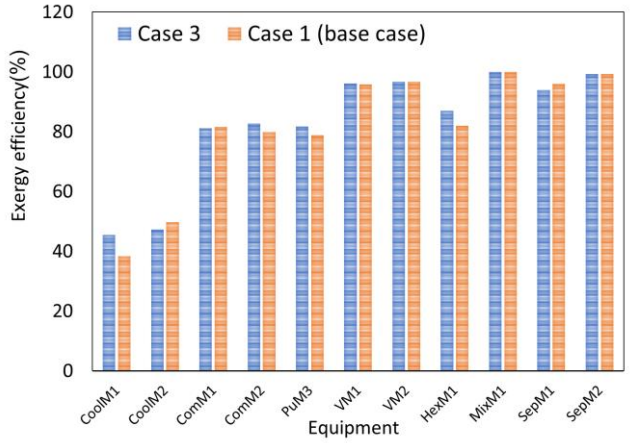


**Fig. 6.2. LNG and LH2 pre-cooling cycle**

**Fig. 6. Exergy efficiency in 3.1: LH2 cooling cycle. 3.2. LNG or LH2 pre-cooling cycle.**

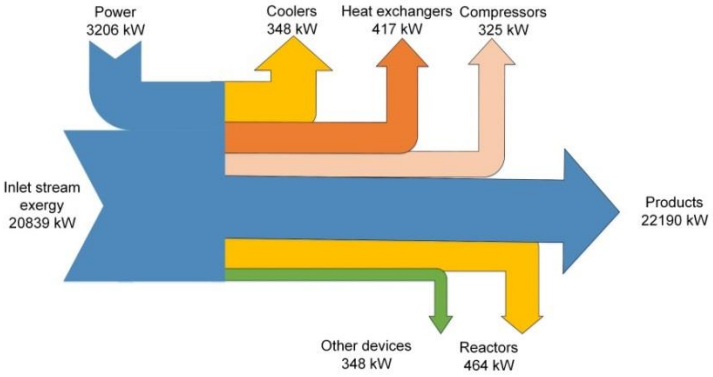


**Fig. 7. Exergy block flow diagram for hydrogen liquefaction cycle.**

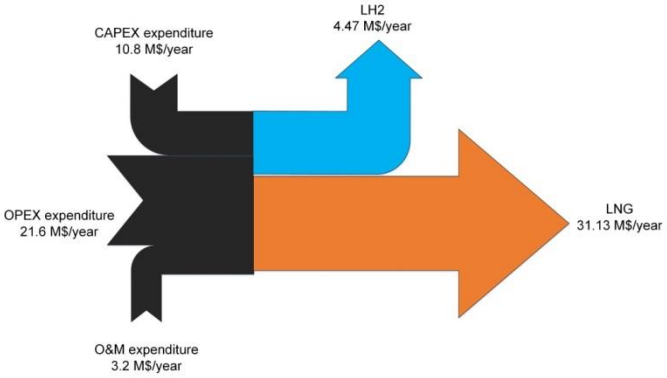


**Fig. 8. Block flow diagram related to overal economic analysis.**

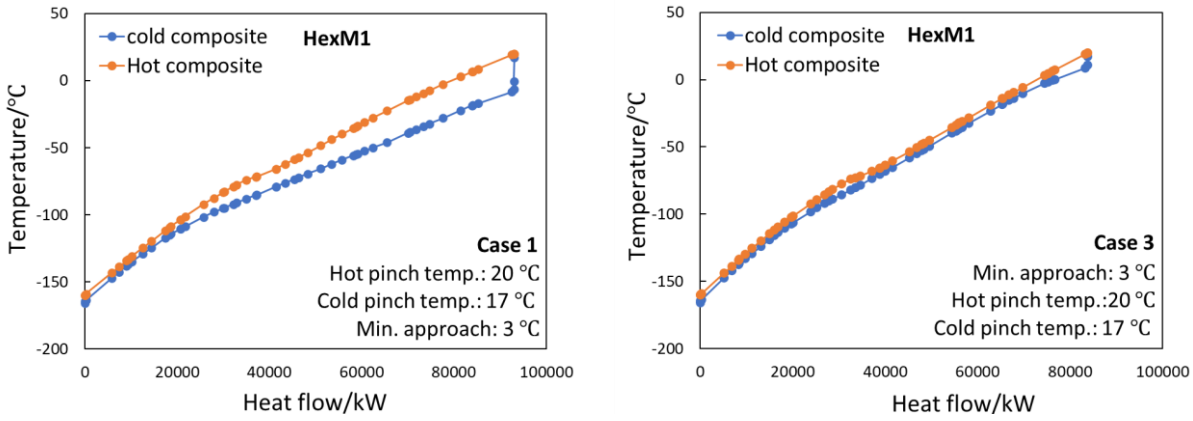


**Fig. 9.1. HexM1 heat exchanger in the pre-cooling part.**

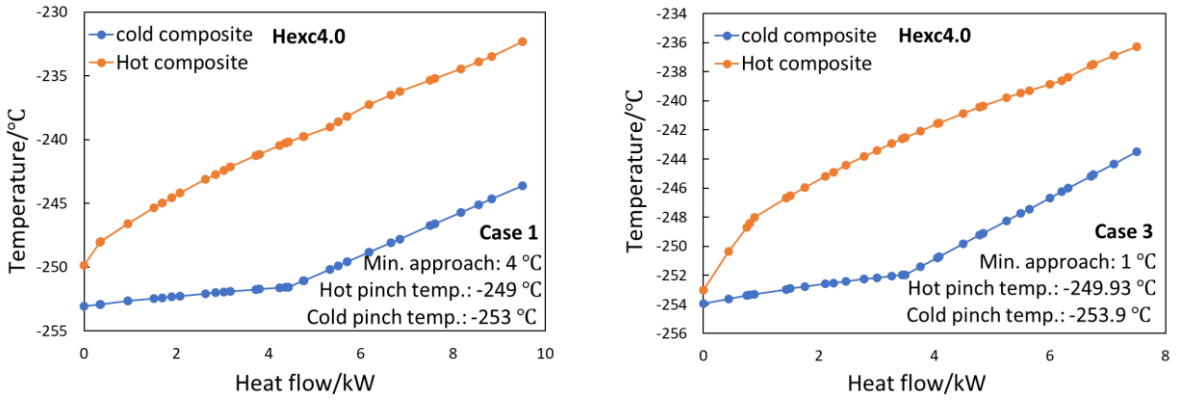


**Fig. 9.2. Hexc4.0 heat exchanger in the cooling part.**

**Fig. 9. Comparison between hot and cold composite curves for two heat exchangers (Fig. 9.1. HexM1, Fig. 9.2. Hexc4.0).**

**Sensitivity analysis**

Fig. 9 shows the composite curves in two heat exchangers that impact the total exergy destruction significantly. The comparison of case 1 and case 3 are shown in Fig. 9.

As shown in Fig. 6 for the natural gas liquefaction cycle or hydrogen pre-cooling part, the HexM1 has the greatest exergy destruction; this device is optimized in Case 3 (final case) by adjusting the minimum temperature approach. The power of compressors in this section for Case 3 (final case) decreases compared to Case 1 (base case), which in turn, results in total power consumption decreasing. Fig. 5.1 shows that the greatest exergy destruction in the cooling part of Case 1 goes to the Hex.c4.0, which has three streams, including one hot and two cold streams. The exergy destruction of this device is reduced in Case 3 in comparison to Case 1. Exergy destruction increased in Case 3 for ortho-para conversion reactors due to inlet temperature changes, but total exergy destruction in Case 3 (final case) is less than that for Case 1(base case). The difference in exergy destruction between Case 3 and Case 1 is 8718 kW. Fig. 6 shows that mixers, pumps, and separators have the slightest exergy destruction compared to other devices. The exergy efficiency of air coolers has the lowest value in the pre-cooling and cooling parts, respectively. The block flow diagram of the inlet and outlet exergy for the hydrogen liquefaction cycle is shown in Fig. 7, additionally, the economic block flow diagram for the overall cycle is shown in Fig. 8.

The low value of the minimum temperature approach in the heat exchangers causes less exergy destruction, but it needs big heat exchangers and much more CAPEX expenditures. In Case 1, the minimum temperature approach range is assumed between 1℃ to 8 ℃. By readjusting the minimum temperature approach in Case 3, it changes to the range of 1℃ to 2 ℃. Of the three cases, Case 3 performs the best in terms of the energy and exergy aspects. In Hexc4.0, the minimum temperature approach is 4℃ and 1 ℃ for Case 1 and Case 3, respectively. In HexM1, the minimum temperature approach is 3℃ as recommended by (Aslambakhsh et al. 2018) in both cases (Case 1 and Case 3), but the two hot and cold composite curves are closer to each other. As shown in Fig. 9, HexM1 with two cold and three hot streams significantly influences the cycle exergy efficiency for the pre-cooling part and the whole cycle.

Sensitivity analysis examines the effect of key variables on the performance of the proposed cycle. In Fig. 10 and Fig. 11, the influence of the maximum pressure of mixed refrigerants on the efficiency of the proposed cycle is investigated for the PRICO cycle and the cooling part of the hydrogen liquefaction cycle.

According to Fig. 10, it is clear that with the maximum pressure in the range of 3300 kPa to 3900 kPa increasing, the SEC reduces, and the COP increases. A pressure of 3900 kPa is the optimal value. Fig. 11 indicates that increasing the maximum pressure of the mixed refrigerant in the cooling part of the hydrogen liquefaction cycle leads to the performance improvement of the hydrogen liquefaction cycle; therefore, the proposed cycle has the best performance at 1100 kPa.

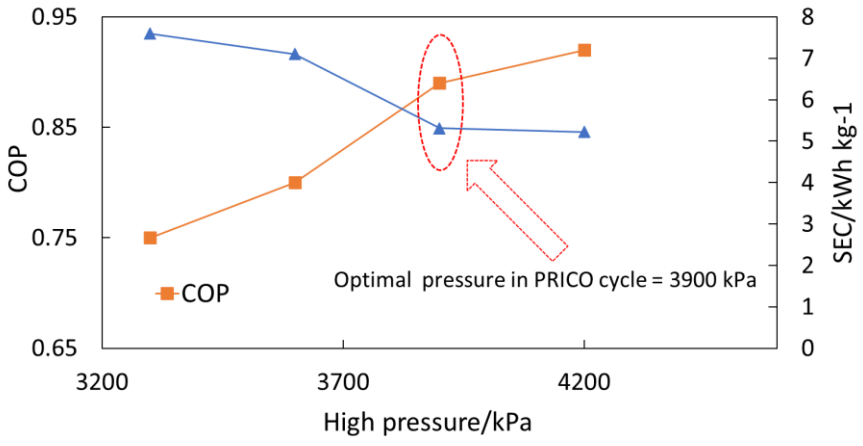


**Fig. 10. High working pressure in the PRICO cycle.**

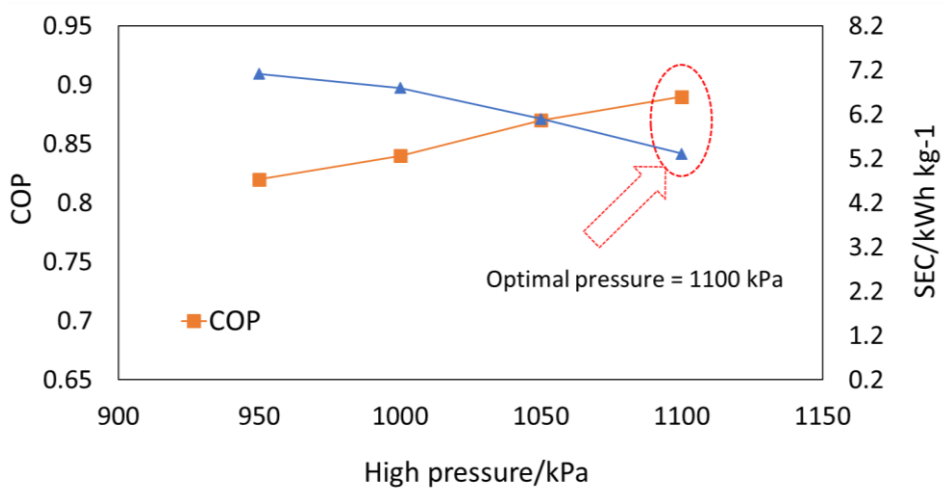


**Fig. 11. Comparison of different high working pressures in the cooling part of the hydrogen liquefaction cycle.**

In Figs. 12 and 13, the effect of the mass flow rate of the mixed refrigerant in the PRICO and cooling part of the hydrogen liquefaction cycle is investigated. As shown in Fig. 12, with the mass flow rate of the mixed refrigerant in the PRICO cycle increasing, SEC decreases significantly, and COP decreases slightly. The same trend is shown in Fig. 13 for the mass flow rate of the mixed refrigerant in the cooling part of the hydrogen liquefaction cycle. A mass flow rate of 354819 kg $h^{-1}$ for the mixed refrigerant of the PRICO cycle results in the best performance of the whole cycle, with the lowest possible flow rate of the mixed refrigerant in the cooling part of the hydrogen liquefaction cycle being 1085 kg $h^{-1}$.

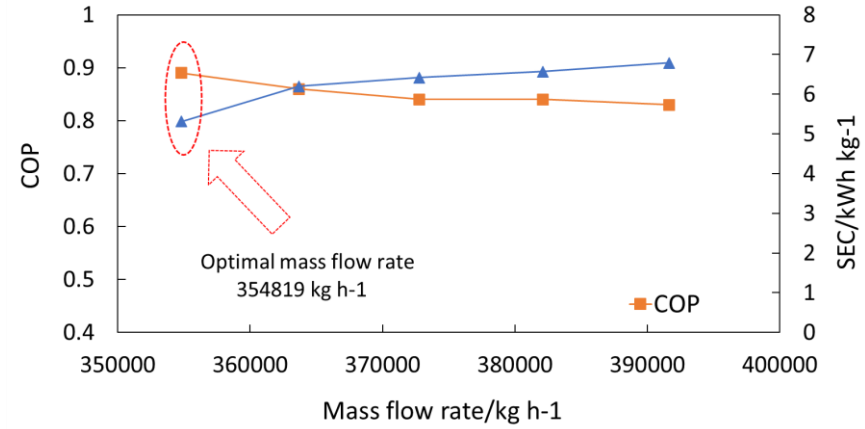


**Fig. 12. Comparison of different mass flow rates of the mixed refrigerant in the PRICO cycle.**

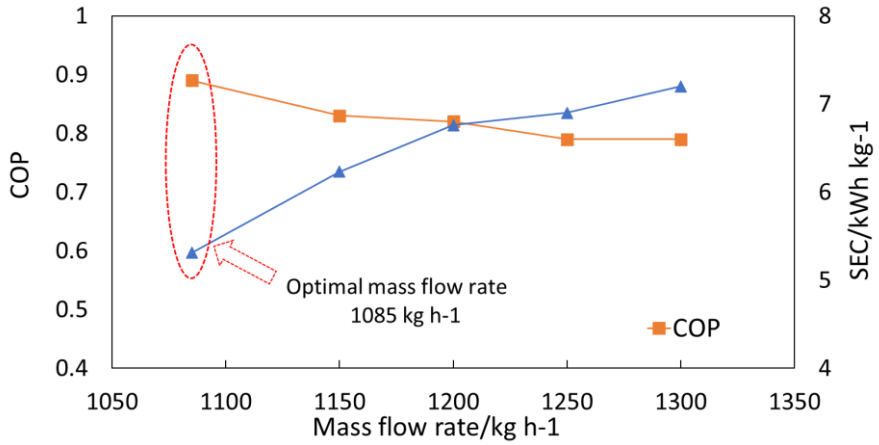


**Fig. 13. Comparison of different mass flow rates of the mixed refrigerant in the cooling part of the hydrogen liquefaction cycle.**

Shown in Figs. 14 and 15 are the influence of the adiabatic efficiency of compressors and expanders on cycle efficiency. As shown in Figs. 15 and 16, the higher the efficiency, the better the cycle efficiency, but the maximum efficiency for expanders and compressors is 85 % in this study as recommended by Berstad et al. (Berstad et al. 2010) and Yin et al. (Yin and Ju 2020a) for mixed refrigerant streams at cryogenic temperatures.

**Economic analysis**

In the following sections, the results of the economic analysis of the proposed cycle are investigated. In the proposed cycle, the annual interest and the payment period are 0.07 and 20 years old, respectively. Fig. 16 shows the different annual expenditures for the proposed cycle (Case 3) and the base case (Case 1).

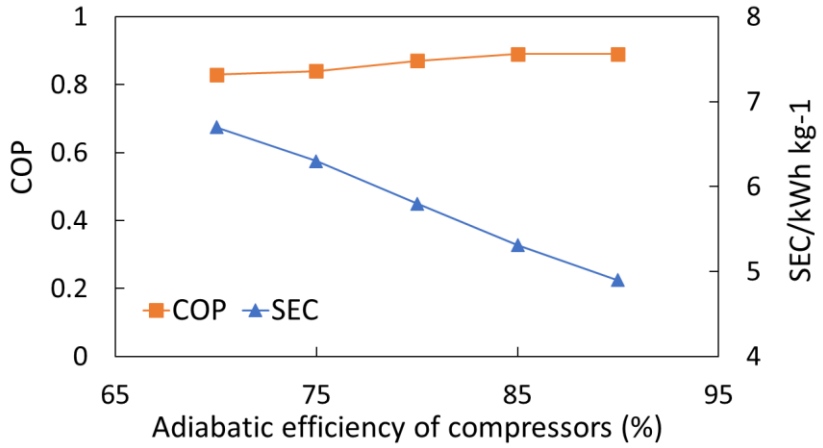


**Fig. 14. Variation of SEC and COP against the adiabatic efficiency of compressors.**

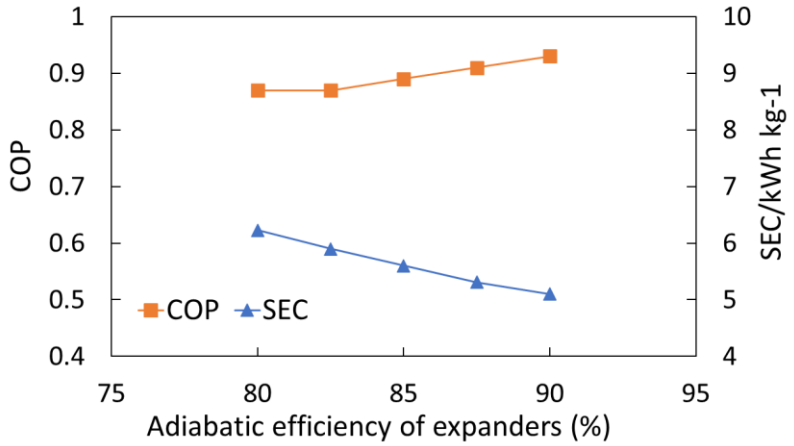


**Fig. 15. Variation of SEC and COP against the adiabatic efficiency of turbine expanders**

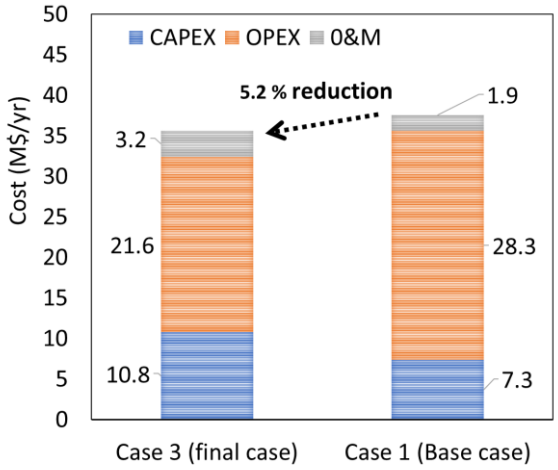


**Fig. 16. CAPEX, OPEX, and O&M expenditures for Case 1 (base case) and Case 3 (final case).**

It can be seen from Fig. 14 that the annual total cost of Case 3 decreases compared to that of Case 1. The main reason for the cost reduction is based on less SEC or power consumption for case 3, in turn, causes the OPEX cost to decrease in comparison to Case 1 significantly. Annual power consumption decreases in Case 3 because the exergy destruction in heat exchangers reduces. In Case 3, the highest rate of expenditure goes to OPEX, consisting of $21.6 million, followed by CAPEX at $10.8 million, and the third rank is allocated to O&M. In Case 1, CAPEX expenditure is $28.3 million, which has a decline in by $6.7 million in case 3. Fig. 17 shows the proportion of the three costs of the proposed cycle. As shown in Fig. 17, the highest cost is assigned to OPEX, making up 61%, which is twice as much as that of CAPEX. Stood at the second rank is CAPEX, consisting of 30%, followed by O&M at 9 % .

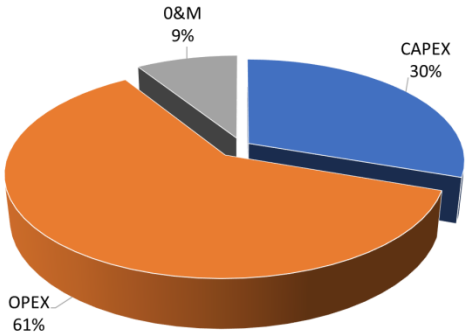


**Fig. 17. The proportion of CAPEX, OPEX, and O&M expenditures for the proposed cycle.**

The performance comparison of the proposed cycle (Case 3 in the present study) and other hydrogen liquefaction cycles is shown in Table 4. SEC of the proposed cycle is 5.31, which has a +25 % improvement compared to the work of (Yin and Ju 2020a). This improvement is based on two main reasons: first, using a suitable mixed refrigerant composition in the hydrogen liquefaction cycle and also utilizing a PRICO cycle in the pre-cooling part of the liquefaction, while the nitrogen refrigeration cycle is used in the pre-cooling part of the model of Yin and Ju's research(Yin and Ju 2020a), and second reason based on that the process integration of the hydrogen liquefaction cycle with an LNG production cycle leads SEC to decrease. In this study, COP and FOM are 0.89 and 0.72, respectively. Table 8 indicates that the proposed cycle has a lower SEC value than that of other cycles mentioned in Table 8. In the work of Mehrpooya et al. (Mehrpooya et al. 2020) a hydrogen liquefaction cycle with an SEC value of 4.16 kwh $kg^{-1}$ was developed, which has a better performance compared to the proposed model in this study. However, they did not consider temperature increase in the ortho-para conversion reactions, which is a major gap, causing a significant difference with experimental results. Consequently, the gap is fixed in this study to achieve close agreement with experimental results.

**Table 8. Performance comparison of the proposed hydrogen liquefaction cycle with the works of Yin and Ju(Yin and Ju 2020a), Yang et al. (Yang et al. 2019), and Berstad et al. (Berstad et al. 2021).**

| Parameters | (Berstad et al. 2010) (Scaled-up) | (Yang et al. 2019) (Scaled-up) | (Yin and Ju 2020a) | Base case (Case 1 in the present study) | Proposed cycle (Case 3 in the present study) |
|---|---|---|---|---|---|
| SEC/**kWh kg$^{-1}$** | 6.57 | 11.05 | 7.13 | 6.13 | 5.31 |
| COP | Not mentioned | Not mentioned | 0.17 | 0.81 | 0.89 |
| FOM | Not mentioned | Not mentioned | 0.49 | 0.67 | 0.72 |
| Net power/**kW** | 413 | 696 | 449 | 385 | 335 |
| LH2 capacity/**kg h$^{-1}$** | 63 | 63 | 63 | 63 | 63 |
| Concentration of para hydrogen in LH2 (%) | 99 | 99 | 99 | 99 | 99 |
| LH2 Pressure/**kPa** | 184 | 130 | 300 | 300 | 300 |
| LH2 temperature/℃ | -251 | -251 | -252 | -251 | -251 |

## 5 Conclusion

High energy consumption in hydrogen and natural gas liquefaction cycles is a crucial problem, which causes high production costs. Using a new design for the hydrogen liquefaction cycle by mixed refrigerant method or integration of the LH2 production cycle with other processes can reduce exergy destruction in equipment; in turn, causing the liquefaction cycle efficiency to increase. In this research, a novel hydrogen liquefaction cycle integrated with an LNG production cycle is proposed. The LH2 production capacity is 1.5 TPD (63 kg $h^{-1}$) TPD. The LNG production cycle is a PRICO cycle with a capacity of 101100 kg $h^{-1}$. Three different mixed refrigerant compositions, including Case1, Case 2, and Case 3, are studied to find the best performance. Case 3 has the best efficiency,

which is proposed as the final model. Three ortho-para conversion reactors are used in this research. SEC is 5.11 for the proposed hydrogen liquefaction cycle, which is +25 % better in terms of SEC than that for a similar cycle mentioned in the literature. COP and FOM of the proposed cycle are 0.89 and 0.72, respectively. Results indicate that the proposed cycle has better performance in comparison to other cycles mentioned in the literature. By performing economic analysis, CAPEX, OPEX, and O&M expenditures are examined for the proposed cycle. Using simultaneous production of LNG and LH2 leads to significant cost reduction in OPEX. In the proposed cycle, the payment period and annual interest are considered 20 years old and 0.07, respectively. The highest cost is assigned to OPEX, making up 61%, which is twice as much as that of CAPEX. The third rank of the total expense is O&M, consisting of 9% of the total annual cost. MBWR and PR EOSs are used to simulate pure hydrogen and mixed refrigerant stream, respectively. Simultaneous using two proper EOSs for the proposed model causes good agreement with experimental results, especially for ortho-para conversion reactions. By using liquid hydrogen as an energy storage method, there is no need to use alternatives with environmental problems, leading to cleaner energy production and sustainable energy. Consumption of hydrogen and natural gas is increasing. By process integration of LNG and LH2 production cycles, the cost of using those fuels can be decreased, which is done in this study. The problem of the high investment cost of hydrogen storage could be solved by considering simultaneous production of LNG and LH2, making it economically viable.

The modified configuration of using two liquefaction cycles in this study is very inspiring and can be used in other liquefaction processes. Furthermore, it is suggested for future works investigate the possibility of adding a renewable power plant to the proposed model to provide renewable power for the compression section of the liquefaction cycle, additionally, by using solar energy and water electrolyzes, LH2 can be produced with zero carbon emission.

## Nomenclature

### Symbols

| | |
|---|---|
| $a_1$ | Pressure cost factor 1 |
| $a_2$ | Pressure cost factor 2 |
| $A_{PFHX}$ | Heat transfer area in heat exchangers($m^2$) |
| $C_{CAPEX}$ | Cost factor |
| $C_{OPEX}$ | Cost of operation($) |
| $C_{O\&M}$ | Operating and maintenance expenditures($) |
| $C_{com}$ | Cost of compressors($) |
| $c_{del}$ | Delivery cost($) |
| $C_{Hex}$ | Cost of heat exchangers ($) |
| $C_{oth}$ | Cost of other equipment ($) |
| $C_{tur}$ | Cost of turbines ($) |
| $Ex$ | Exergy (kW) |
| $e^{ch}$ | Chemical exergy(kW) |
| $e^{ph}$ | Physical exergy(kW) |
| $f_{p,hex}$ | The pressure cost factor in heat exchangers |
| $h$ | Specific enthalpy (kJ $kg^{-1}$) |
| $HP$ | Work of compressor or turbine(kW) |
| $\dot{m}_l$ | Mass flow rate (kg $h^{-1}$) |
| $P_{net}$ | Total power consumption in a cycle(kW) |
| $Q_{cv}$ | Heat transfer (kW) |
| $I$ | Exergy destruction(kW) |
| $I_a$ | Annual interest rate |
| $s$ | Specific entropy (kJ $kg^{-1}°C^{-1}$) |
| $t$ | Payment period(year) |
| $W$ | Work(kW) |

### Abbreviations

| | |
|---|---|
| CAPEX | CAPEX |
| COP | COP |
| EOS | EOS |
| FOM | FOM |
| LH2 | LH2 |
| LNG | Liquid natural gas |
| MBWR | Modified Benedict-Webb-Rubin |
| OPEX | Operation expenses |
| O&M | Operating and maintenance expenditure |
| SEC | Specific energy consumption (kWh $kg^{-1}$) |

### Greek letter

| | |
|---|---|
| η | Exergy efficiency |

## Reference


Aasadnia, Majid, Mehdi Mehrpooya, and Hojat Ansarinasab. 2019. "A 3E Evaluation on the Interaction between Environmental Impacts and Costs in a Hydrogen Liquefier Combined with Absorption Refrigeration Systems." *Applied Thermal Engineering* 159. doi: 10.1016/j.applthermaleng.2019.113798.

Aasadnia, Majid, Mehdi Mehrpooya, and Bahram Ghorbani. 2021. "A Novel Integrated Structure for Hydrogen Purification Using the Cryogenic Method." *Journal of Cleaner Production* 278. doi: 10.1016/j.jclepro.2020.123872.

Ahmed, Tarek. 2016. *Equations of State and PVT Analysis: Applications for Improved Reservoir Modeling: Second Edition*.

Akrami, Ehsan, Arash Nemati, Hossein Nami, and Faramarz Ranjbar. 2018. "Exergy and Exergoeconomic Assessment of Hydrogen and Cooling Production from Concentrated PVT Equipped with PEM Electrolyzer and LiBr-H2O Absorption Chiller." *International Journal of Hydrogen Energy* 43(2). doi: 10.1016/j.ijhydene.2017.11.007.

Andrews, John W. 2020. "Hydrogen Production and Carbon Sequestration by Steam Methane Reforming and Fracking with Carbon Dioxide." *International Journal of Hydrogen Energy* 45(16). doi: 10.1016/j.ijhydene.2020.01.231.

Ansarinasab, Hojat, Mehdi Mehrpooya, and Milad Sadeghzadeh. 2019. "An Exergy-Based Investigation on Hydrogen Liquefaction Plant-Exergy, Exergoeconomic, and Exergoenvironmental Analyses." *Journal of Cleaner Production* 210:530–41. doi: 10.1016/j.jclepro.2018.11.090.

Aslambakhsh, Amir Hamzeh, Mohammad Ali Moosavian, Majid Amidpour, Mohammad Hosseini, and Saeedeh AmirAfshar. 2018. "Global Cost Optimization of a Mini-Scale Liquefied Natural Gas Plant." *Energy* 148:1191–1200. doi: 10.1016/j.energy.2018.01.127.

Babu, V. 2019. *Fundamentals of Engineering Thermodynamics*.

Berstad, David O., Jacob H. Stang, and Petter Nekså. 2010. "Large-Scale Hydrogen Liquefier Utilising Mixed-Refrigerant Pre-Cooling." *International Journal of Hydrogen Energy* 35(10). doi: 10.1016/j.ijhydene.2010.02.001.

Berstad, David, Geir Skaugen, and Øivind Wilhelmsen. 2021. "Dissecting the Exergy Balance of a Hydrogen Liquefier: Analysis of a Scaled-up Claude Hydrogen Liquefier with Mixed Refrigerant Pre-Cooling." *International Journal of Hydrogen Energy* 46(11):8014–29. doi: 10.1016/j.ijhydene.2020.09.188.

Cardella, U., L. Decker, and H. Klein. 2017. "Roadmap to Economically Viable Hydrogen Liquefaction." *International Journal of Hydrogen Energy* 42(19):13329–38. doi: 10.1016/j.ijhydene.2017.01.068.

Cardella, U., L. Decker, J. Sundberg, and H. Klein. 2017. "Process Optimization for Large-Scale Hydrogen Liquefaction." *International Journal of Hydrogen Energy* 42(17):12339–54. doi: 10.1016/j.ijhydene.2017.03.167.

Chang, Ho Myung, Ki Nam Ryu, and Jong Hoon Baik. 2018. "Thermodynamic Design of Hydrogen Liquefaction Systems with Helium or Neon Brayton Refrigerator." *Cryogenics* 91:68–76. doi: 10.1016/j.cryogenics.2018.02.007.

Dewar, James. 1898. "Liquid Hydrogen: Preliminary Note on the Liquefaction of Hydrogen and Helium." *Science* 8(183). doi: 10.1126/science.8.183.3.

Donaubauer, Philipp J., Umberto Cardella, Lutz Decker, and Harald Klein. 2019. "Kinetics and Heat Exchanger Design for Catalytic Ortho-Para Hydrogen Conversion during Liquefaction." *Chemical Engineering and Technology* 42(3):669–79. doi: 10.1002/ceat.201800345.

Faramarz Ranjbar, Arash Nourbakhsh Saadabad, Mahdi Nami Khaliledeh, Saman Faramarzi, Farhad Firouzy. 2022. "Simulation, Analysis and Optimization of a Non-Emission Process Producing Power, Hydrogen Gas and Liquid Hydrogen Using Solar Energy and PEM Electrolysis." *Journal of Mechanical Engineering* 02(04):26–48.

Faramarzi, Saman, Mostafa Mafi, SMM Nainiyan, and Ramin Ghasemiasl. 2021. "Modification of a Fuel Peak-Shaving System in Shahid Mofateh Power Plant." PP. 56–60 in *The 29th Annual International Conference of the Iranian Association of Mechanical Engineers and the 8th Conference on Thermal Power Plants*.

Faramarzi, Saman, Seyed Mojtaba Mousavi Nainiyan, Mostafa Mafi, and Ramin Ghasemiasl. 2021. "Genetic Algorithm Optimization of Two Natural Gas Liquefaction Methods Based on Energy, Exergy, and Economy Analyses: The Case Study of Shahid Rajaee Power Plant Peak-Shaving System." *Gas Processing* 9(1):91–108. doi: 10.22108/GPJ.2021.126527.1097.

Faramarzi, Saman, Seyed Mojtaba Mousavi Nainiyan, Mostafa Mafi, and Ramin Ghasemiasl. 2021. "Modification and Optimization of an Integrated Hydrogen Liquefaction Process with an LNG Regasification System." *Journal of Mechanical Engineering*. doi: 10.22034/jmeut.2021.44570.2842.

Faramarzi, Saman, Seyed Mojtaba Mousavi Nainiyan, Mostafa Mafi, and Ramin Ghasemiasl. 2021a. "A Novel Hydrogen Liquefaction Process Based on LNG Cold Energy and Mixed Refrigerant Cycle." *International Journal of Refrigeration*. doi: 10.1016/j.ijrefrig.2021.07.022.

Faramarzi, Saman, Seyed Mojtaba Mousavi Nainiyan, Mostafa Mafi, and Ramin Ghasemiasl. 2021. "Proposing a Simultaneous Production Cycle of Liquid Natural Gas and Liquid Hydrogen." PP. 67–71 in *The 29th Annual International Conference of the Iranian Association of Mechanical Engineers and the 8th Conference on Thermal Power Plants*.

Fratzscher, W. 1997. "The Exergy Method of Thermal Plant Analysis." *International Journal of Refrigeration*. doi: 10.1016/s0140-7007(97)85546-6.

Ghorbani, B., G. R. Salehi, M. Amidpour, and M. H. Hamedi. 2012. "Exergy and Exergoeconomic Evaluation of Gas Separation Process." *Journal of Natural Gas Science and Engineering* 9:86–93. doi: 10.1016/j.jngse.2012.05.001.

Ghorbani, Bahram, Armin Ebrahimi, Sajedeh Rooholamini, and Masoud Ziabasharhagh. 2020. "Integrated Fischer-Tropsch Synthesis Process with Hydrogen Liquefaction Cycle." *Journal of Cleaner Production*. doi: 10.1016/j.jclepro.2020.124592.

Ghorbani, Bahram, Armin Ebrahimi, Fatemeh Skandarzadeh, and Masoud Ziabasharhagh. 2020. "Energy, Exergy and Pinch Analyses of an Integrated Cryogenic Natural Gas Process Based on Coupling of Absorption–Compression Refrigeration System, Organic Rankine Cycle and Solar Parabolic Trough Collectors." *Journal of Thermal Analysis and Calorimetry*. doi: 10.1007/s10973-020-10158-3.

Ghorbani, Bahram, Zahra Javadi, Sohrab Zendehboudi, and Majid Amidpour. 2020. "Energy, Exergy, and Economic Analyses of a New Integrated System for Generation of Power and Liquid Fuels Using Liquefied Natural Gas Regasification and Solar Collectors." *Energy Conversion and Management* 219. doi: 10.1016/j.enconman.2020.112915.

Ghorbani, Bahram, Mehdi Mehrpooya, Majid Aasadnia, and Malek Shariati Niasar. 2019. "Hydrogen Liquefaction Process Using Solar Energy and Organic Rankine Cycle Power System." *Journal of Cleaner Production* 235:1465–82. doi: 10.1016/j.jclepro.2019.06.227.

Ghorbani, Bahram, Sohrab Zendehboudi, and

Mostafa Moradi. 2021. "Development of an Integrated Structure of Hydrogen and Oxygen Liquefaction Cycle Using Wind Turbines, Kalina Power Generation Cycle, and Electrolyzer." *Energy* 221:119653. doi: 10.1016/j.energy.2020.119653.

Hammad, Anwar, and Ibrahim Dincer. 2018. "Analysis and Assessment of an Advanced Hydrogen Liquefaction System." *International Journal of Hydrogen Energy* 43(2):1139–51. doi: 10.1016/j.ijhydene.2017.10.158.

Hosseini, Seyed Ehsan, and Brayden Butler. 2020. "Design and Analysis of a Hybrid Concentrated Photovoltaic Thermal System Integrated with an Organic Rankine Cycle for Hydrogen Production." *Journal of Thermal Analysis and Calorimetry*. doi: 10.1007/s10973-020-09556-4.

Jacob W. Leachman, Richard T Jacobsen, Eric W. Lemmon, and Steven G. Penoncello. 2017. *Thermodynamic Properties of Cryogenic Fluids*. second. Cham: Springer.

Kaşka, Önder, Ceyhun Yılmaz, Onur Bor, and Nehir Tokgöz. 2018. "The Performance Assessment of a Combined Organic Rankine-Vapor Compression Refrigeration Cycle Aided Hydrogen Liquefaction." *International Journal of Hydrogen Energy* 43(44). doi: 10.1016/j.ijhydene.2018.07.092.

Kotas, T. J. 1985. "Exergy Analysis of Simple Processes." Pp. 99–161 in *The Exergy Method of Thermal Plant Analysis*. Elsevier.

Krasae-In, Songwut, Arne M. Bredesen, Jacob H. Stang, and Petter Neksa. 2011. "Simulation and Experiment of a Hydrogen Liquefaction Test Rig Using a Multi-Component Refrigerant Refrigeration System." *International Journal of Hydrogen Energy* 36(1):907–19. doi: 10.1016/j.ijhydene.2010.09.005.

Lin, Wensheng, Xiaojun Xiong, and Anzhong Gu. 2018. "Optimization and Thermodynamic Analysis of a Cascade PLNG (Pressurized Liquefied Natural Gas) Process with CO2 Cryogenic Removal." *Energy* 161. doi: 10.1016/j.energy.2018.07.051.

Mafi, Mostafa. 2015. "Development in Mixed Refrigerant Cycles for Separation Systems of Petrochemical Industries and Thermo-Economical Optimization through Combined Pinch and Exergy Analysis." PhD thesis, K. N. Toosi University of technology.

Mafi, Mostafa, S. M.ostafa Mousav. Naeynian, and M. Amidpour. 2009. "Exergy Analysis of Multistage Cascade Low Temperature Refrigeration Systems Used in Olefin Plants." *International Journal of Refrigeration* 32(2). doi: 10.1016/j.ijrefrig.2008.05.008.

Marmolejo-Correa, Danahe, and Truls Gundersen. 2012. "A Comparison of Exergy Efficiency Definitions with Focus on Low Temperature Processes." *Energy* 44(1):477–89. doi: 10.1016/j.energy.2012.06.001.

Mazyan, W., A. Ahmadi, H. Ahmed, and M. Hoorfar. 2016. "Market and Technology Assessment of Natural Gas Processing: A Review." *Journal of Natural Gas Science and Engineering* 30:487–514. doi: 10.1016/j.jngse.2016.02.010.

Mehrpooya, Mehdi, Masoud Kalhorzadeh, and Mahmood Chahartaghi. 2016. "Investigation of Novel Integrated Air Separation Processes, Cold Energy Recovery of Liquefied Natural Gas and Carbon Dioxide Power Cycle." *Journal of Cleaner Production* 113. doi: 10.1016/j.jclepro.2015.12.058.

Mehrpooya, Mehdi, Mirhadi S. Sadaghiani, and Nader Hedayat. 2020. "A Novel Integrated Hydrogen and Natural Gas Liquefaction Process Using Two Multistage Mixed Refrigerant Refrigeration Systems." *International Journal of Energy Research* 44(3):1636–53. doi: 10.1002/er.4978.

Mokarizadeh Haghighi Shirazi, M., and D. Mowla. 2010. "Energy Optimization for Liquefaction Process of Natural Gas in Peak Shaving Plant." *Energy* 35(7). doi: 10.1016/j.energy.2010.03.018.

Mokhatab, Saeid, John Y. Mak, Jaleel V. Valappil, and David A. Wood. 2013. *Handbook of Liquefied Natural Gas*.

Morosuk, T., S. Tesch, A. Hiemann, G. Tsatsaronis, and N. Bin Omar. 2015. "Evaluation of the PRICO Liquefaction Process Using Exergy-Based Methods." *Journal of Natural Gas Science and Engineering* 27. doi: 10.1016/j.jngse.2015.02.007.

Nouri, Milad, Morteza Miansari, and Bahram Ghorbani. 2020. "Exergy and Economic Analyses of a Novel Hybrid Structure for Simultaneous Production of Liquid Hydrogen and Carbon Dioxide Using Photovoltaic and Electrolyzer Systems." *Journal of Cleaner Production* 259:120862. doi: 10.1016/J.JCLEPRO.2020.120862.

Ram B. Gupta, Angelo Basile, and T. Nejat Veziroglu. 2013. *Compendium of Hydrogen Energy Volume 2: Hydrogen Storage, Distribution and Infrastructure*. Vol. 53.

Rezaei, Mostafa, Ali Mostafaeipour, Mojtaba Qolipour, and Mozhgan Momeni. 2019. "Energy Supply for Water Electrolysis Systems Using Wind and Solar Energy to Produce Hydrogen: A Case Study of Iran." *Frontiers in Energy* 13(3). doi: 10.1007/s11708-019-0635-x.

Sabbagh, Omid, Mohammad Ali Fanaei, and Alireza Arjomand. 2020. "Optimal Design of a Novel NGL/LNG Integrated Scheme: Economic and Exergetic Evaluation." *Journal of Thermal Analysis and Calorimetry*. doi: 10.1007/s10973-020-10126-x.

Serio, L., J. Bremer, S. Claudet, D. Delikaris, G. Ferlin, M. Pezzetti, O. Pirotte, L. Tavian, and U. Wagner. 2015. "CERN Experience and Strategy for the Maintenance of Cryogenic Plants and Distribution Systems." in *IOP Conference Series: Materials Science and Engineering*. Vol. 101.

Tan, Hongbo, Siyu Shan, Yang Nie, and Qingxuan Zhao. 2018. "A New Boil-off Gas Re-Liquefaction System for LNG Carriers Based on Dual Mixed Refrigerant Cycle." *Cryogenics* 92:84–92. doi:

10.1016/j.cryogenics.2018.04.009.

Utlu, Zafer, and Arif Karabuga. 2021. "Conventional and Enhanced Exergy Analysis of a Hydrogen Liquefaction System." *International Journal of Hydrogen Energy* 46(2). doi: 10.1016/j.ijhydene.2020.10.104.

Valenti, Gianluca, Ennio MacChi, and Samuele Brioschi. 2012. "The Influence of the Thermodynamic Model of Equilibrium-Hydrogen on the Simulation of Its Liquefaction." *International Journal of Hydrogen Energy* 37(14):10779–88. doi: 10.1016/j.ijhydene.2012.04.050.

Wu, Jitan, and Yonglin Ju. 2020. "Comprehensive Comparison of Small-Scale Natural Gas Liquefaction Processes Using Brazed Plate Heat Exchangers." *Frontiers in Energy* 14(4). doi: 10.1007/s11708-020-0705-0.

Xu, Xiongwen, Jinping Liu, Chuanshuo Jiang, and Le Cao. 2013. "The Correlation between Mixed Refrigerant Composition and Ambient Conditions in the PRICO LNG Process." *Applied Energy* 102:1127–36. doi: 10.1016/J.APENERGY.2012.06.031.

Yang, Jae Hyeon, Younggak Yoon, Mincheol Ryu, Su Kyung An, Jisup Shin, and Chul Jin Lee. 2019. "Integrated Hydrogen Liquefaction Process with Steam Methane Reforming by Using Liquefied Natural Gas Cooling System." *Applied Energy* 255. doi: 10.1016/j.apenergy.2019.113840.

Yilmaz, Ceyhun, and Onder Kaska. 2018. "Performance Analysis and Optimization of a Hydrogen Liquefaction System Assisted by Geothermal Absorption Precooling Refrigeration Cycle." *International Journal of Hydrogen Energy* 43(44). doi: 10.1016/j.ijhydene.2018.08.019.

Yin, Liang, and Yonglin Ju. 2020a. "Process Optimization and Analysis of a Novel Hydrogen Liquefaction Cycle." *International Journal of Refrigeration* 110:219–30. doi: 10.1016/j.ijrefrig.2019.11.004.

Yin, Liang, and Yonglin Ju. 2020b. "Review on the Design and Optimization of Hydrogen Liquefaction Processes." *Frontiers in Energy* 14(3):530–44.

Zhang, Jinrui, Hans Meerman, René Benders, and André Faaij. 2020. "Comprehensive Review of Current Natural Gas Liquefaction Processes on Technical and Economic Performance." *Applied Thermal Engineering* 166.

Zhao, Yanxing, Maoqiong Gong, Haocheng Wang, Hao Guo, and Xueqiang Dong. 2020. "Development of Mobile Miniature Natural Gas Liquefiers." *Frontiers in Energy* 14(4).

Zhuzhgov, A. V., O. P. Krivoruchko, L. A. Isupova, O. N. Mart'yanov, and V. N. Parmon. 2018. "Low-Temperature Conversion of Ortho-Hydrogen into Liquid Para-Hydrogen: Process and Catalysts. Review." *Catalysis in Industry* 10(1). doi: 10.1134/S2070050418010117.